

Models and hardware implementation of methods of Pre-processing Images based on the Cellular Automata

Stepan Bilan

Faculty "Infrastructure and rolling stock of railways", State Economy and Technology University of Transport, Kiev, Ukraine
bstepan@ukr.net

ABSTRACT

The paper deals with the organization and construction of cellular automata for the implementation of the basic operations of the pre-processing images. The methods of edge detection, zoom, filling inside area of images and also selection of objects are considered. The analysis of the impact of different forms of the neighboring cells for the effective execution of operations is carried. Programs that simulate the operation of CA are developed. Computer models of the main elements in CAD Active-HDL have been obtained by modeling the structure of the CA. The obtained models have passed the test and their analysis showed high reliability of operation. This allows us to implement them in modern CPLD and FPGA hardware. This hardware is easily reprogrammed under the given structure of CA. Implementing FPGAs allows us to use one chip for realization of the basic functions of the CA. The experimental results showed that the used methods and CA are highly effective. The use of CA allows to describe of the image with high speed highly effective.

Keywords: Cellular automata, image, contour, zoom, filling inside area.

1 Introduction

All existing methods and tools for image recognition are divided into two main stages: stages of learning and recognition. Both processes are tied to the need of efficient representation and are optimal for forming an image. For advanced information technologies and computational tools the signals and images are presented in the form of codes, which values describe as an image. Therefore there is a need exists for effective methods and means, which describe an input image. Due to the variety of images and the complexity of geometric shapes and the parameters, different sets of features are used. These sets divide all images into classes. These sets of characteristic features are created by the developers and consist of different amounts.

However, each characteristic feature of different nature and requires specialized methods and tools to determine its quantitative values. In this case, for the selection of characteristic features, a great number of operations are used. The main ones are the operations of edge detection, scaling, noise removal, segmentation, selection of the objects, etc. For realization of such operations various methods and tools are used, as well as researches of new modern approaches for their effective implementation are conducted. Improvement of the performance of such operations allow cellular automata (CA), which have a unified structure, to reduce the time of operations [1-6].

2 Detection of Images Edges in CA

Edge detection operation is one of the main from image preprocessing operations. Edges analysis allows to describe of geometric shape of image of the selected object in the visual scene. Different

methods of the edges selecting are known of object, which is described in [2, 5, 7, 8, 9, 10]. However, the most effective tools that allow you to detect an edge in one cycle, are CA [2, 7]. CA allows you to implement edge detection for various organizations of cell neighborhoods (fig. 1).

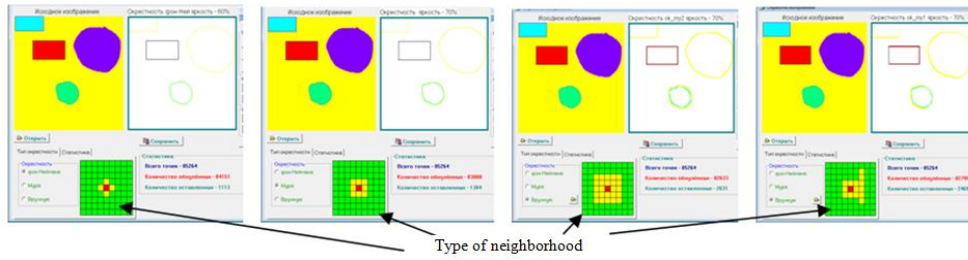


Figure 1: Example of edge detection simulation in CA

Thus, the increasing of neighborhoods order is causes by changes in thickness of the edge line. Therefore, for easing of processing of edge cells it is better to use von Neumann or Moore neighborhood. The cells function of such CA for neighborhood of the von Neumann can be represented by the following relationship

$$b(t+1) = \begin{cases} b(t), & \text{if } x_1(t) \wedge x_2(t) \wedge x_3(t) \wedge x_4(t) = 0, \\ 0, & \text{if } x_1(t) \wedge x_2(t) \wedge x_3(t) \wedge x_4(t) = 1 \end{cases} \quad (1)$$

where $x_1(t)$, $x_2(t)$, $x_3(t)$, $x_4(t)$ - the signals at the outputs of neighborhood cells (top, right, bottom, left) at time t ; $b(t)$ - state of a cell at time t .

For Moore neighborhood the model (1) will contain eight signals from neighborhood cells

$$b(t+1) = \begin{cases} b(t), & \text{if } x_1(t) \wedge x_2(t) \wedge \dots \wedge x_8(t) = 0 \\ 0, & \text{if } x_1(t) \wedge x_2(t) \wedge \dots \wedge x_8(t) = 1 \end{cases} \quad (2)$$

As we can see from the illustrated example it is possible to create a shadow of the object, to make some lines thicker, and the others are thinner. Through variation of the neighborhood structure we can create different shapes and transformation of the objects contours.

However, for halftone image processing and edge detection of the object it is necessary to use thresholding processing. The CA separates cells of object from the background on the base of selected threshold value of brightness. Each cell is determined its the mean value from value set of cells of the neighborhood and is compared with a predetermined threshold value. If the value exceeds the control cell threshold, this cells belongs to the cells of the edge. Otherwise, the cell is set to value of background (fig. 2).

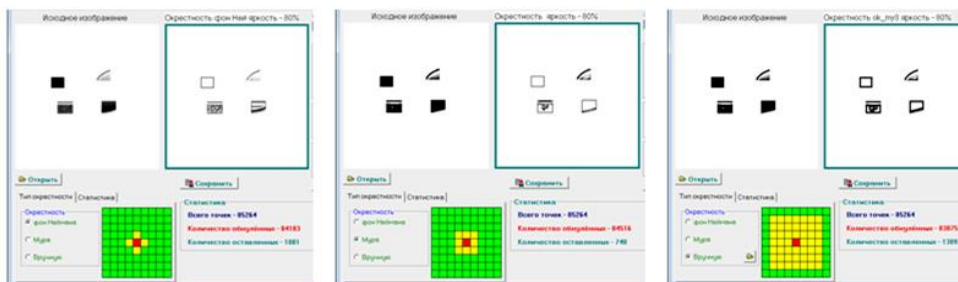


Figure 2: Example of edge detection of halftone image

Threshold variation value allows to select edge as well as to implement noise filtering, which presented in the image. Also, this approach allows the edges selection of images by gradations of brightness.

Cell structure, which implements the CA for edge detection of the halftone image is submitted on figure 3.

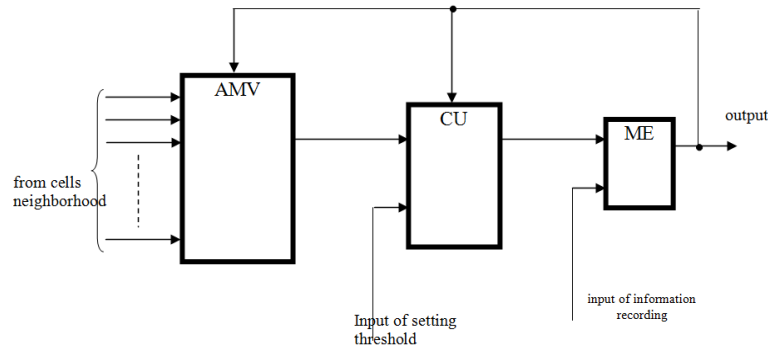


Figure 3: Structural circuit of one cells of CA for edge detection

Cell contains a memory element (ME), comparing unit (CU) and the adder of mean value (AMV) that summarizes values of the neighborhood cells and determines the average value. CU compares it with a predetermined threshold value and with code from output of the ME, and accordingly controls the state of ME.

For all the selected types of neighbors their comparative analysis was performed by number of cells that form edges.

Graph of cell contour distribution for the neighborhood of von Neumann, Moore, of the second and third orders is shown in Figure 4.

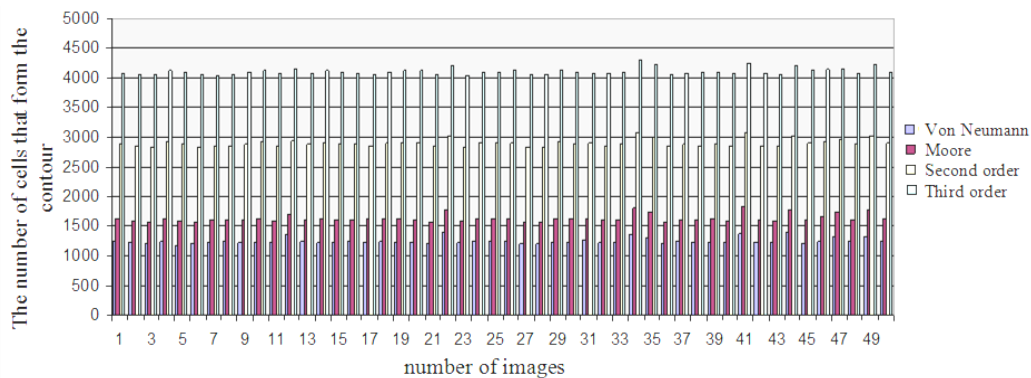


Figure 4: Graph of cell contour distribution for the neighborhood of von Neumann, Moore, of the second and third orders

The analysis of the dependency shows the stability of the difference between the numbers of cells that form the edges. At the same time shape of the curves are the same for all types of neighborhoods at the same sample of images, which have been investigated.

The experiments were conducted for symmetric structures of neighborhoods that have the same shape but different in the number of cells that form the neighborhood.

In the next part of the experimental research real images of figures obtained by photographing were used.

The resulting image was divided into separate images of the equal dimension (300×300). At the same time each figure was rotated on a certain angle.

For the contrast selection and binarization of the resulting images boundaries with effective sensitivity were defined where unneeded cells were completely removes, which did not belong to the figure. For existing an image binarization with sensitivity in the range from 50 to 60 percent was carried out. Image processing was carried out by the program "Study". Histograms of cells that form the edges of the figures images for given forms of neighborhood are shown in Figure 5.

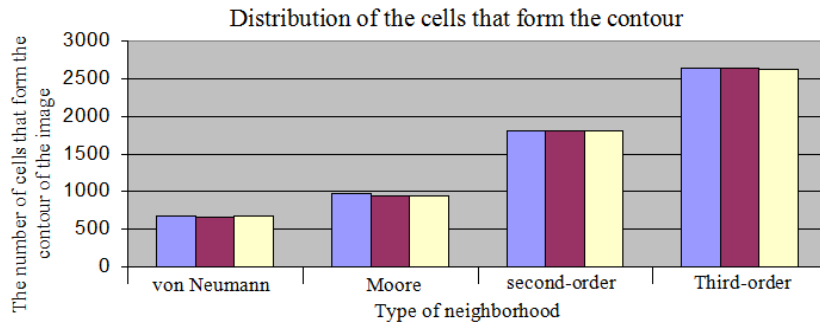


Figure 5: Histograms of edge cells of images for selected types of neighborhoods

With the help of these experiments average values of the ratios of the number of cells that form a contour for different types of neighborhoods were obtained. The relations obtained show that the difference between the obtained values of the ratio to ratio of real images and the computer images, practically negligible. Consequently, all depends on the accurate initial morphological image processing by the camera.

3 Scaling of images in CA

There are many problems in the known image scaling methods that are associated with the assignment of the center of scaling and arbitrary scaling factors for X and Y coordinates [10, 11]. CA allows to solve these problems.

The method is described below:

Initially, a cell is selected, which is the center of scaling. Each cell of CA is given by a scaling factor K_M . The value K_M is determined. If $K_M > 1$ cell reproduction begins with shift on both coordinates in turn. The closest cells to the central cell first begin to reproduce. The other cells and their values shift. The first cell creates additional cells on one of the coordinates with the same conditions. Their number is K_M . The other cells and their values shift on the K_M of cells from the cell of scaling center (figure 6).

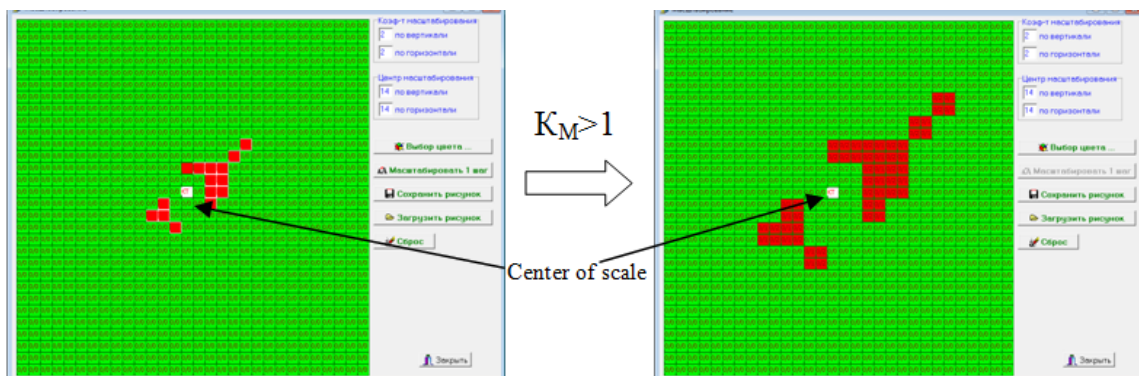


Figure 6: Example of scaling images based on CA

When all of the cells and their values on one coordinate proliferate in opposite sides from the cell of scaling center, cells reproduction begins according to another coordinate. The reproduction is carried out similarly. At different scaling factors for different coordinates also the image changes in the direction of these coordinates (see figure 7).

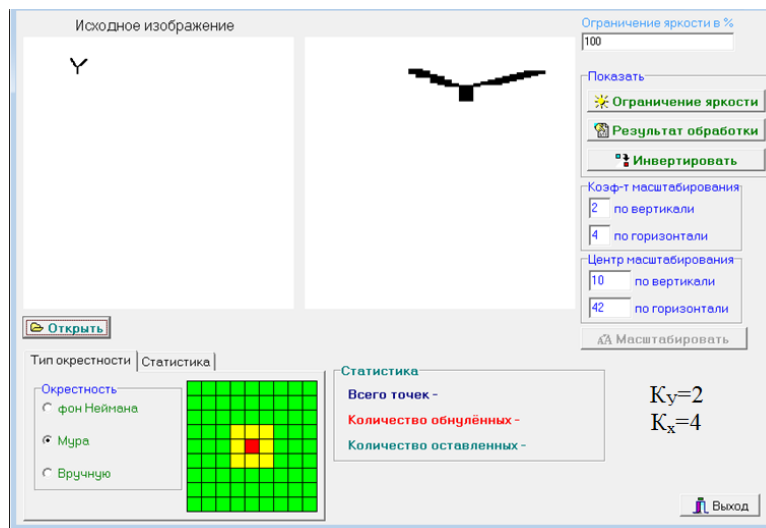


Figure 7: Example of scaling images based on CA with different KM

If $K_M < 1$, then the cells are absorbed in the direction to the cell in the center of scaling. The first absorbed cells are the neighboring cells with equal values, which are adjacent to the central cell. Their number is equal to K_M . Other cells and their values shift to the center on the value K_M of cells. After the first absorption the cells with another state begin to absorb. These cells are located after the first absorbed cells. This process continues until the complete enumeration of all the cells on one coordinate, and then on the other.

Model of the scaling process description can be divided into two models that describe the functioning of the cell for increase or to decrease of the image. Each of these models takes into account the three components.

- States of a cell at time t for one of the coordinates $b_i(t)$.
- Availability of excitation signal $e_i(t)_{excite}$.
- The scale ratio value recorded in this cell.

Model describing the cell behavior for process of the image increase on the X-axis in the one direction is the following

$$\frac{b_i^x(t+1)}{K_i^M(t+1)} = \begin{cases} \frac{b_{i-1}^x(t)}{K_i^M(t) + K_{i-1}^M(t)}, & \text{if } b_i^x(t) = b_{i-1}^x(t), e_{i-1}^x(t)_{excite} = 1 \\ \frac{b_i^x(t)}{0}, & \text{if } b_i^x(t) = b_{i+1}^x(t), e_i^x(t)_{excite} = 1, \\ \frac{b_i^x(t)}{0}, & \text{if } b_i^x(t) \neq b_{i+1}^x(t), e_i^x(t)_{excite} = 1, s_{i+1}^x(t)_{shift} = 1, K_i^M(t) > 0 \\ \frac{b_{i-1}^x(t)}{K_i^M(t) - 1}, & \text{if } b_{i-1}^x(t) \neq b_i^x(t), e_{i-1}^x(t)_{excite} = 0, K_i^M(t) > 0, s_{i+1}^x(t)_{shift} = 1, \\ \frac{b_{i-1}^x(t)}{K_{i-1}^M(t)}, & \text{if } e_{i-1}^x(t)_{excite} = 0, K_{i-1}^M(t) = 0, s_{i-1}^x(t)_{shift} = s_{i+1}^x(t)_{shift} = 1 \\ \frac{b_{i-1}^x(t)}{K_{i-1}^M(t)}, & \text{if } b_{i+1}^x - \text{does not exist}, e_{i-1}^x(t)_{excite} = e_i^x(t)_{excite} = 0, s_{i-1}^x(t)_{shift} = 1 \\ \frac{b_{i-1}^x(t)}{0}, & \text{if } b_{i+1}^x - \text{does not exist}, e_{i-1}^x(t)_{excite} = 1, K_{i-1}^M(t) > 0 \end{cases}, \quad (3)$$

where $\frac{b_i^x(t+1)}{K_i^M(t+1)}$ - the status value of the cell (numerator) at time (t +1) and the value of scaling factor (the denominator) of cell, which is i-th cell on the X coordinate of the cell selected as the center of scaling;

$e_i^x(t)_{excite}$ - the value on output of formation of a excitation signal of the cell at time t, which is the i-th cell on the X coordinate of the cell selected as the center of scaling;

$s_{i+1}^x(t)_{shiff}$ - Signal, which allows record values of the state of the i-th cell in the (i +1)-th cell.

In the numerator of the model internal state of the cell is described, and the denominator represents the value of the scaling factor.

The first row in (3) describes the increase in the neighboring cells $b_i^x(t)$, which have the state, and the i-th cell is selected from the center of scaling becomes excited. An example of such a situation is shown in Figure. 8.

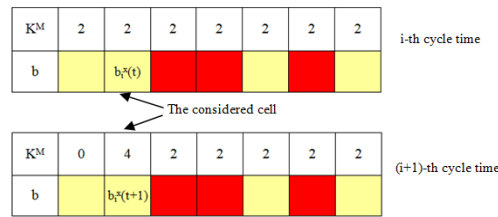


Figure 8: Example of the cell functioning in a situation as described in the first row of model (3)

Second row of model (3) describes the transmission of the excitation signal next adjacent cell (Fig. 9), which is in the same state as the cell excitation.

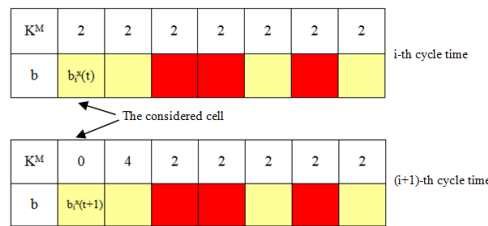


Figure 9: Example of excitation signal transmission

The third row of the model (3) shows that the i-th cell records its state in (i +1)-th cell (Fig. 10).

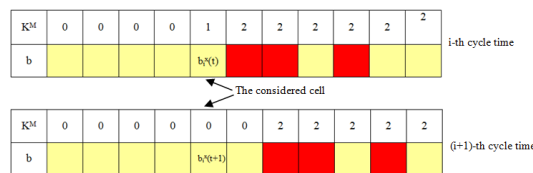


Figure 10: Example implementation of the model (3) according to an embodiment of the third row

The fourth row describes the transition of state of i-th cell into the state (i-1)-th cell. State of the i-th cell is transferred to the (i +1)-th cell (Fig. 11).

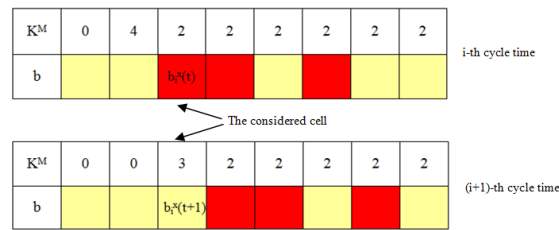


Figure 11: Implementation example of the fourth row in model (3)

The fifth line describes a behavior cell in case of shift of its state from cell center of scaling (Fig. 12).

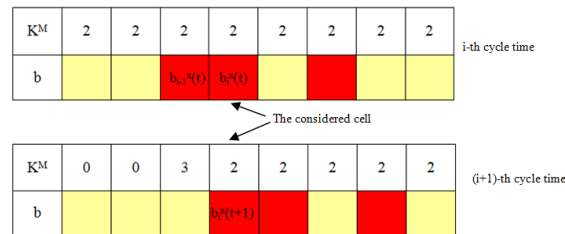


Figure 12: An example of transmitting state of the cell, which is not excited

The sixth and seventh rows describe the behavior of the boundary cells of CA.

At the initial time every cell records a value K^M , which decremented by 1 ($K^M - 1$).

Thus, the excited state of the cells at each time step is transferred to the next neighboring cells, if $K^M(t) > 0$. The number of such cells is equal K^M .

The cell states are recorded in the following neighboring cells, if they received shift signals from two neighboring cells (shift of cell states in the direction from the cell, which is the center of scaling). Installing cells in readiness to shift is carried out by distribution shift signal from the center cell of scaling. The direction of propagation of this signal indicates the direction of the shift.

The excitation signal is generated at the next adjacent cell based on a specified condition

$$e_i(t+1)_{excite} = \begin{cases} 1, & \text{if } K_{i-1}^M(t) = 0, e_{i-1}(t)_{excite} = 1 \\ 1, & \text{if } b_i(t) = b_{i-1}(t), e_{i-1}(t)_{excite} = 1, \\ 0, & \text{in other cases} \end{cases} \quad (4)$$

To zoom out, of an image the absorption cell states are used. Cells are absorbed in each row and by each coordinate. Initially are absorbed cells along the X-coordinate and then along the Y coordinate. The model describing the functioning of the cells in direction X coordinate has the form

$$\frac{b_i^x(t+1)}{K_i^M(t+1)} = \begin{cases} \frac{b_i^x(t)}{K_i^M - 1}, & \text{if } e_i^x(t)_{excite} = 1, b_i^x(t) = b_{i+1}^x(t), \\ \frac{b_{i+1}^x(t)}{K_{i+1}^M(t)}, & \text{if } e_{i-1}^x(t)_{excite} = 1, K_{i-1}^M(t) > 0, b_i^x(t) \neq b_{i+1}^x(t), b_i^x(t) = b_{i-1}^x(t), s_i^x(t)_{shift} = 0, \\ \frac{b_{i+1}^x(t)}{K_{i+1}^M(t)}, & \text{if } e_i^x(t)_{excite} = e_{i-1}^x(t) = 0, s_{i-1}^x(t)_{shift} = s_i^x(t) = 1 \\ 0, & \text{if } e_i^x(t)_{excite} = 1, b_i^x(t) = b_i^x(t+1) \\ \frac{b_i^x(t)}{0}, & \text{if } b_{i+1}^x(t) \text{ - does not exist} \end{cases} \quad (5)$$

The first row describes the behavior of cells in the case when the next adjacent cell from the excited cells has the same state (Fig. 13).



Figure 13: Example of the cell functioning which describes in the first row of the model (5)

The second row describes the shift of cells in row in direction the neighboring excited cells (Fig. 14).

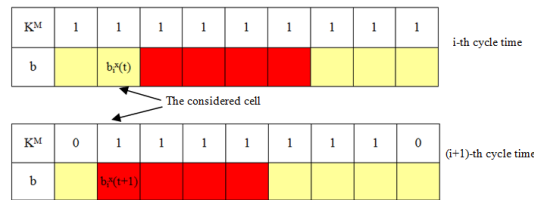


Figure 14: Example of the shift of cell states

The third row of model (5) describes the shift of the contents of all cells in the direction of the excited cells. In this case, the cells are not have excitation cell among adjacent cells (Figure 15).

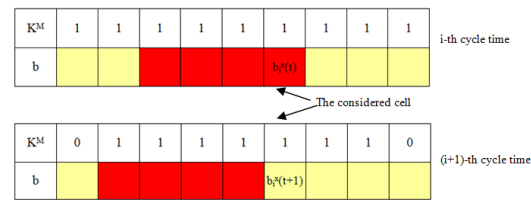


Figure 15: Example of the shift excited states of a cell without adjacent excitation cells

The fourth row describes the process of absorption by one cell its adjacent cells with equal state (Figure 16).

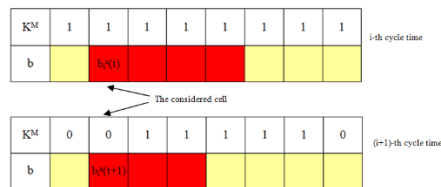


Figure 16: Example of absorption of the cell

If state of the cell is shifted or absorbed, then this cell generates the shift signal $s(t)_{shift}$ to neighboring cells.

The excitation signal is generated at the next adjacent cell based on a specified condition

$$e_i(t+1)_{excite} = \begin{cases} 1, & \text{if } K_{i-1}^M(t) = 0, e_{i-1}(t)_{excite} = 1, b_{i-1}(t) = b_i(t) \\ 1, & \text{if } b_{i-1}(t) \neq b_i(t), e_{i-1}(t)_{excite} = 1 \\ 0, & \text{in other cases} \end{cases}, \quad (6)$$

An example scaling operation on every cycle time is represented by Figure 17.

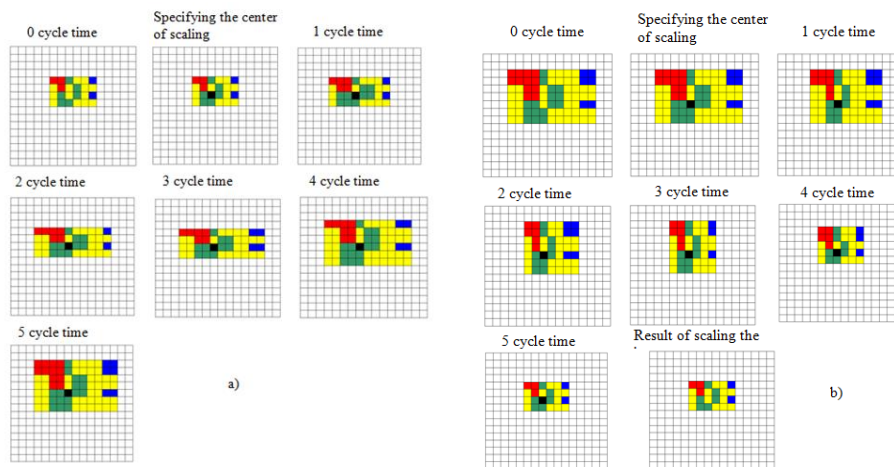


Figure 17: Example of a detailed image scaling: a – scaling with $K^M > 1$, b – scaling with $K^M < 1$

According to the proposed methods a program was created that implements them on the basis of models of CA functioning. Examples of scaling of real images by program are shown in Figure 18.

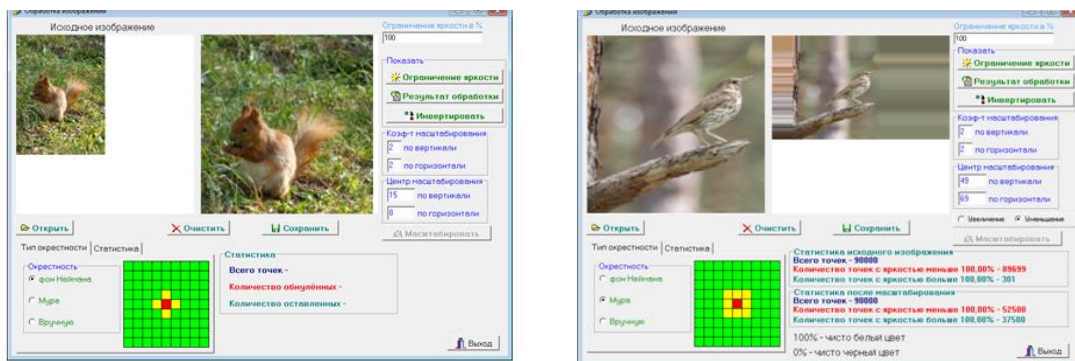


Figure 18: Example of scaling images based on CA

For accurate and reliable research of scaling figures were formed, which consisted of units of cells. Small number of cells that forms the image of figures was used for the precise counting them during zooming.

At the time of the research of cells scaling algorithm was carried out by counting the number of cells that form the image after applications of each zoom level. Histogram of cells distribution on the images of figures with equal amounts of cells, which form the primary image is shown in Figure 19.

Obtained dependence shows that the number of cells, which is obtained when the zoom factor is increased on 1, increases in four times, and when the zoom factor is 3, the number of cells increases in 16. The dependence shows an increase of cells numbers in four times more than K_M .

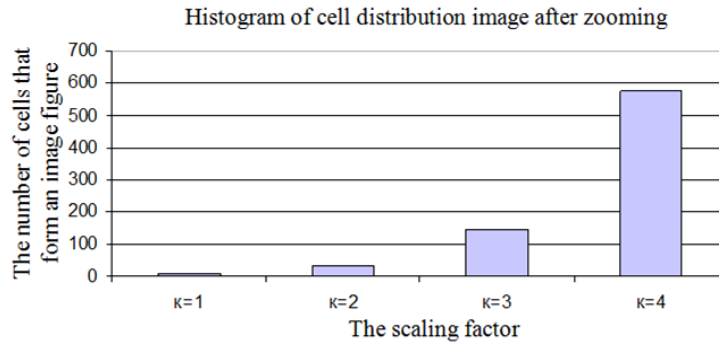


Figure 19: Histograms of cells distribution contour of figures for specific types of neighborhood

4 Filling in CA

Reverse operation for edge detection is operation of filling of inside area of image boundary. These operations have differences under time expenses. If edges have been selected during one clock cycle in the CA, time of operation of area filling depends on the number of CA cells that make up the inner area of the contour.

Known methods of parity control and seed cells are successfully implemented in the CA. However, the implementation of parity control method complicates the structure of the cells due to the need to eliminate false results at the presence of extreme peaks and horizontal lines (fig. 20). The implementation of the method of the seed pixel cells simplifies the cell structure and requires to define the inner area (fig. 21).

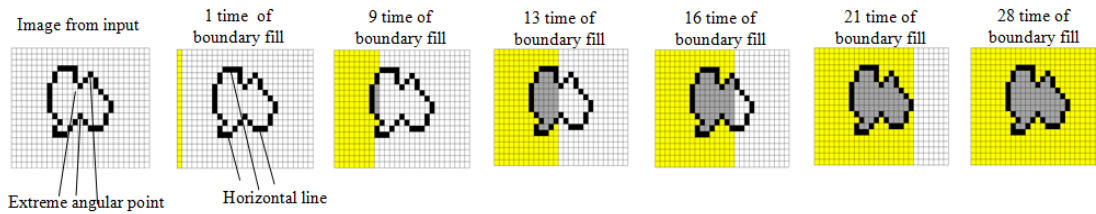


Figure 20: Example of implementation of the parity control method

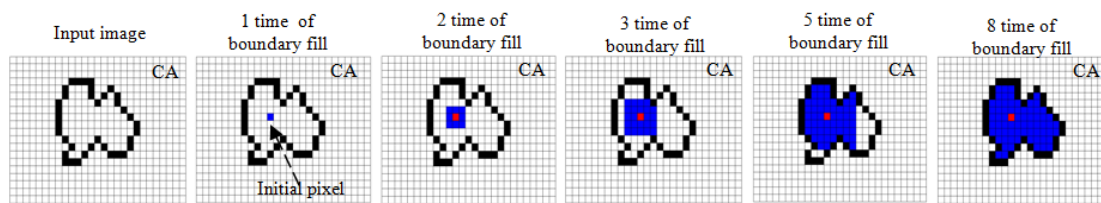


Figure 21: Example of implementation of the parity control method

Example of implementation of the seed cells method.

To implement the parity control method the following model is used.

$$b_i(t+1) = \begin{cases} b_{i-1}(t), & \text{if } b_i(t) = a(t)_{backgr}, e_i(t)_{excite} = 1, b_{i-1}(t) \neq a(t)_{backgr}, F_i(t)_{extreme} = 1, X_i(t)_{even} = 1, \\ b_i(t), & \text{in othe cases} \end{cases} \quad (7)$$

where

$$F_i(t)_{extreme} = [x_i(t)_{LUP} \vee x_i(t)_{C.UP} \vee x_i(t)_{R.UP}] \wedge [x_i(t)_{L.B} \vee x_i(t)_{C.B} \vee x_i(t)_{R.B}], \quad (8)$$

$$X_i(t+1)_{even} = \overline{X_{i-2}(t)} \wedge X_{i-1}(t) \wedge F_{i-1}(t)_{extreme} \wedge \overline{X_i(t)} \vee X_{i-2}(t) \wedge X_{i-1}(t) \wedge \overline{F_{i-2}(t)_{extreme}} \wedge \overline{X_i(t)} \wedge F_i(t)_{extreme} \quad (9)$$

$a(t)_{backgr}$ - the value of the background brightness;

$X_i(t)$ - the output signal of the i-th cell at time t;

$x_i(t)_{even}$ - the value of the signal of paired values of edge in the i-th cell one row CA (1 – is odd intersection of contour, 0 - a multiple of two);

$x_i(t)_{LUP}, x_i(t)_{CUP}, x_i(t)_{RUP}$ - the signals states of cells that present left, center and right upper cells of the Moore neighborhood for a given cell at time t;

$x_i(t)_{L.B}, x_i(t)_{C.B}, x_i(t)_{R.B}$ - the signals states of cells that present left, center and right bottom cells of the Moore neighborhood for a given cell at time t.

The model describes the operation of the single cell of CA in row. The signals at the outputs of the neighborhood cells and their state at the appropriate time are taken into account.

For filling of the image by seed cell method we uses the model

$$b_i(t+1)_{excit} = \begin{cases} 1, & \text{if } Q_i(t)_{neugh}^{excit} = 1, b_i(t) = a(t)_{backgr} \\ b_i(t), & \text{if } Q_i(t)_{neugh}^{excit} = 0, \\ b_i(t) & b_i(t) = 1, Q_i(t)_{neugh}^{excit} = 1 \end{cases} \quad (10)$$

where $Q_i(t)_{neugh}^{excit} = \bigvee_{j=1}^n b_j(t)_{excit}$ - indicates the presence of the excited cells in the neighborhood of the i-th cell, which has the state 1;

$b_j(t)_{excit}$ - the output signal of j-th cell of neighborhood, which is in an excited state;

n – the number of cells, which form a neighborhood;

$b_i(t+1)_{excit}$ - the state of the cell, which is in an excited state at time t+1.

The values originally recorded in cells must be fixed and have a certain state after filling. Considering this, the cell has the structure shown in Figure 22.

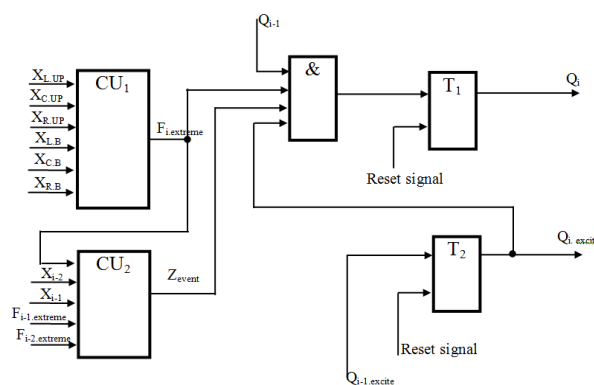


Figure 22: Scheme of cell, which eliminates situations of a false filling of areas that do not belong to the image

T_1 is intended for recording an image, and T_2 – for supporting of the filling process (trigger of excitation). Control units (CU_1 and CU_2) are provide control of T_1 trigger state.

On the scheme the output status i-th cell is shown Q_i , and the output of the excitation signal - $Q_{i.excite}$.

The main condition is that in the contour of image should not be any discontinuities, because this leads to errors in the implementation of the method. Organization of cells of the medium is based on the two triggers, one of which is used to store information about the boundary, and the second - to fill of area.

For a hardware implementation of the method of seed cells, each cell has additional trigger (T_c) of the initial installation. In the state "1", the edge cells will be initially. The speed of the filling process of an image depends on the right choice of cell. Filling time is also reduced with an increasing number of seed cells.

Functional scheme of the cell is shown in Figure 23.

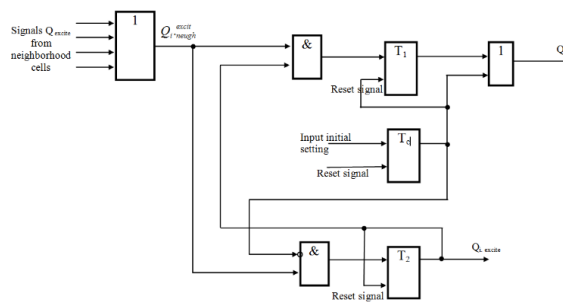


Figure 23: Functional scheme of cell to implement the method of the seed cells

Implementation of these methods in CA absentia reduces time costs; their conjugation allows halftone filling based on the location of the radiation source.

The second method is faster than the first. The speed increase allows using of several initial image elements which fill the inner area. However, the initial cell is mounted inside the area which is defined by the user in advance. This is a drawback of the second method.

5 System Structure of Image Recognition on the Base of CA

The considered operation of images pretreatment are ones of the basic operations, which allow to simplify the methods of selection of the information characteristic features. Use of CA allows to combine the group of CA for all operations in one CA. The structure of cell of generalized CA is shown in Figure 24.

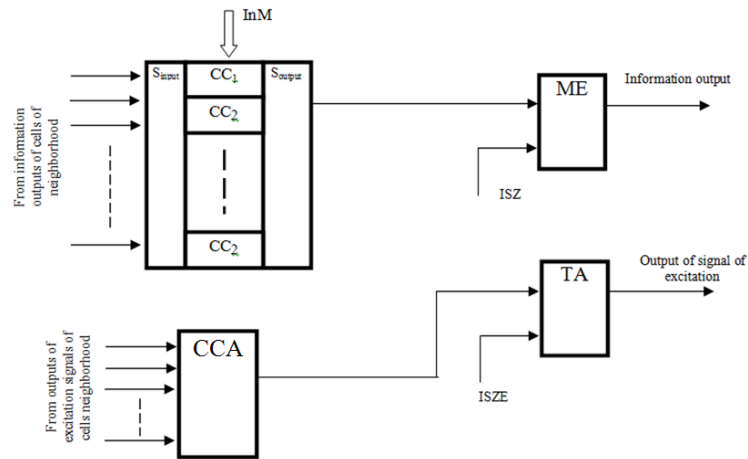


Figure 24: Functional scheme of cell of generalized CA

One cell of a generalized CA consists of memory element (ME) and control scheme of its condition (CSC). CSC consists of n combinational circuits (CC), which are combined on the common inputs by switcher inputs (S_{input}) from the outputs of cells that belong to the neighborhood. The outputs of each CC are connected to the inputs of the switch outputs (S_{output}). Its total output is connected to the control input of the state of ME. Through the control input (InM) selects the CC, which must operate at a given time.

Each CC has a structure, which realizes a necessary operation (edges selection, scaling, filling, etc.), and its output at a predetermined timing is connected to a common output. Signal from the output CSC controls the state of ME.

This structure allows to simplify CA and by switching of CC to reach different sequences of operations. To extending the number of operations performed by the CA an additional trigger of arousal (TA) and an appropriate combinational circuit (CCA), which processes the signal from output of the TA of neighborhood cell are introduced in each cell. Availability of TA allowed to implement an operation specified by cells, where TA are in a single state. The excitation signal is transmitted between neighboring cells. Introduction of additional TA allows to divide the processes of performing of different operations to prepare images. Cell structure for CA, which implements the described operations, were modeled in CAD Active-HDL and showed reliable operation. The resulting model can be easily implemented in modern FPGAs.

After performing operations of previous selection the operation of the main characteristic features definition is conducted and a vector of numerical values of attributes is formed. This vector describes the image on input of recognition system. The requirements are imposing as to the location and quantitative characteristics. One of the approaches to description of the images on the digital and the analog level is described in the works [2, 12]. This method implements the functioning of the system as an analogue of the human optic canal at the level of the waveform.

Block - circuit of the system processing and recognition is presented in Figure 25.

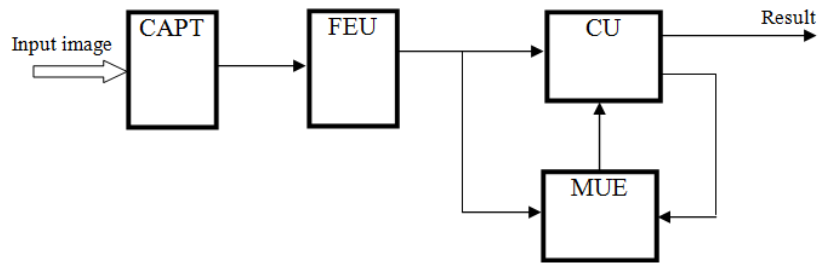


Figure 25: Structure of system of processing and recognition of image

The system comprises CA of pretreatment (CAPT), feature extraction unit (FEU), the memory unit of etalons (MUE) and a comparison unit (CU). CAPT processing the input image and FEU selects the characteristic features. At the output FEU vector of numeric values of attributes, which describe the image is formed. One of the variants of FEU is presented in the works of [2, 12, 13]. The code of vector is supplied to a first input of the CU, which performs the comparison with the etalon code vector. Etalon vector is supplied to the second input of the CU from the output MUE. If the code of etalon does not match to the code of input image, the CU generates a signal on the second output, which is fed to the second input of MUE. MUE carries out is forming of the next closest code of etalon, etc. If the code is not found, the code of the input image is assigned an identifier and it is stored in the MUE through the first input. The system recognizes the image and learns during functioning.

6 Conclusion

All operations are implemented on the CA, which implement asynchronous signal propagation of excitation in the field of CA. The excited cells perform the selected operation and conduct an analysis of cells of their own neighborhood. This approach made possible to perform operations in the individual cells of a field of CA and expanded the number of different operations, which are performed simultaneously.

As a result of the executed experiments on the basis of computer simulation high efficiency of use CA is proved. The developed tools allow to specify the shape of the surrounding area and the thickness of the contour, and to choose an arbitrary scaling center. Besides the method allows to specify different coefficients for each coordinate, which allows to set the appropriate image transformation. By the individual customization of CA efficient extracting of the necessary features performed, which enable optimal description of both simple and complex images.

REFERENCES

- [1]. Von Neumann, J. Theory of Self-Reproducing Automata: Edited and completed by A. Burks. University of Illinois Press, 1966.
- [2]. Belan S., Specialized cellular structures for image contour analysis, Cybernetics and Systems Analysis, 2011. 47(5): p. 695-704.
- [3]. Wolfram S., Cellular Automata. Los Alamos Science, 1983. 9: p. 2-21.
- [4]. Belan S., and Motornyyuk R., Extraction of characteristic features of images with the help of the radon transform and its hardware implementation in terms of cellular automata. Cybernetics and Systems Analysis, 2013. 49(1): p. 7-14.

- [5]. Ioannidis K., Andreadis I. Sirakoulis G. Ch. An Edge Preserving Image Resizing Method Based on Cellular Automata. Springer-Verlag, Berlin Heidelberg, ACRI2012, LNCS, 749, 2012. 375-384.
- [6]. Bandini, S., Bonomi, A., Vizzari, G. An Analysis of Different Types and Effects of Asynchronicity in Cellular Automata update Schemes. *Natural Computing*, 2012. 11(2): p. 277-287.
- [7]. Kozhemyako V., Belan S., Savaliuk I. (1997). Optoelectronic self – regulation neural system for treatment of vision information. *SPIE Proceedings*, Wasington, USA, 1997. 3055, p. 120-126.
- [8]. Chen M.J., Huang C.H., Lee W.L. (2005). A fast edge-oriented algorithm for image interpolation. *Image and Vision Computing*, 2005. (23): p. 791–798.
- [9]. Canny J. A computational approach to edge-detection. *IEEE Trans. Pattern Anal. Mach. Intell*, 1986. (8), p. 679–700.
- [10]. Wolfram S. *Theory and applications of Cellular Automata*. World Scientific, Singapore, 1986.
- [11]. Amanatiadis A., Andreadis I., Gasteratos, A. A Log-Polar interpolation applied to image scaling. In: *IEEE International Workshop on Imaging Systems and Techniques*, Cracovia, Poland, 2007, p. 1–5.
- [12]. Cha Y., Kim S. The error-amended sharp edge (EASE) scheme for imaging zooming. *IEEE Trans. Image Process*, 2007. (16), p. 1496–1505.
- [13]. Belan S., Belan N. *Temporal-Impulse Description of Complex Image Based on Cellular Automata*. Springer-Verlag Berlin Heidelberg. PaCT2013, LNCS.- 2013. 7979. 291-295.